

1 **Title**

2 **DAWDLE interacts with DICER-LIKE proteins to mediate small RNA biogenesis**

3 Shuxin Zhang^{1*}, Yongchao Dou^{2,†}, Shengjun Li², Guodong Ren³, David Chevalier⁴, Chi Zhang²
4 and Bin Yu^{2*}

5

6 ¹: State Key Laboratory of Crop Biology, College of Life Sciences, Shandong Agricultural
7 University, Taian, Shandong 271018, China

8 ²:Center for Plant Science Innovation & School of Biological Sciences, University of Nebraska-
9 Lincoln, Lincoln, Nebraska 68588-0666, USA

10 ³: State Key Laboratory of Genetic Engineering and Collaborative Innovation Center for
11 Genetics and Development, School of Life Sciences, Fudan University, Shanghai 200438, China

12 ⁴: Department of Biological Sciences, East Georgia State College, Swainsboro, Georgia 30401,
13 USA

14

15 [†]: Current Address: Department of Molecular and Human Genetics & Lester and Sue Smith
16 Breast Center, Baylor College of Medicine, Houston, TX 77030

17

18 *: Corresponding author:

19 Shuxin Zhang

20 Tel: 86-538-8244008

21 Email: sxzhang@sdau.edu.cn

22

23 Bin Yu

24 Tel: 402-472-2125

25 Email: byu3@unl.edu

26 **One-sentence summary:** DAWDLE modulates small RNA processing through its interaction
27 with DCL proteins.

28 **Author Contributions**

29 S.Z. and B.Y. designed the experiments and prepared the manuscript. S.Z., S.L., Y.D., G.R.,
30 D.C., and C.Z. performed the experiments. S.Z. and B.Y. analyzed the data.

31

32 **Short title: DAWDLE in small RNA biogenesis**

33 **Key word: DAWDLE, miRNA, siRNA, protein-protein interaction, Arabidopsis**

34

35 **Abstract**

36 DAWDLE (DDL) is a conserved forkhead-associated (FHA) domain-containing protein with
37 essential roles in plant development and immunity. It acts in the biogenesis of microRNAs
38 (miRNAs) and endogenous small interfering RNAs (siRNAs), which regulate gene expression at
39 the transcriptional and/or post-transcriptional levels. However, the functional mechanism of
40 DDL and its impact on exogenous siRNAs remain elusive. Here we report that DDL is required
41 for the biogenesis of siRNAs derived from sense transgenes and inverted-repeat transgenes.
42 Furthermore, we show that a mutation in the FHA domain of DDL disrupts the interaction of
43 DDL with DICER-LIKE1 (DCL1), which is the enzyme that catalyzes miRNA maturation from
44 primary miRNA transcripts (pri-miRNAs), resulting in impaired pri-miRNA processing.
45 Moreover, we demonstrate that DDL interacts with DCL3, which is a DCL1 homolog
46 responsible for siRNA production, and this interaction is crucial for optimal DCL3 activity.
47 These results reveal that the interaction of DDL with DCLs is required for the biogenesis of
48 miRNAs and siRNAs in *Arabidopsis*.

49

50 **Introduction**

51 Small RNAs (sRNAs) including microRNAs (miRNAs) and small interfering RNAs (siRNAs)
52 play multiple roles in regulating many biological processes by mediating transcriptional or post-
53 transcriptional gene silencing (Baulcombe, 2004; Axtell, 2013). miRNAs and siRNAs are
54 chemically indistinguishable (Zhang *et al.*, 2015). However, miRNAs are processed from
55 primary miRNA transcripts (pri-miRNAs) that contain one or more miRNA-residing imperfect
56 stem-loops, while siRNAs originate from long perfect double-stranded RNAs that are often the
57 products of the RNA-dependent RNA polymerase (RDR) (Voinnet, 2009). Upon production,
58 miRNAs and siRNAs join the effector protein called ARGONAUTE (AGO) to silence genes

59 containing complementary sequences through cleavage of a target transcript, translational
60 inhibition and/or chromatin modification (Baulcombe, 2004; Vaucheret, 2008; Voinnet, 2009).

61
62 Based on their origin, endogenous siRNAs can be further classified into three different classes:
63 siRNAs generated from repeated DNAs such as transposons (ra-siRNAs), phased-siRNAs (pha-
64 siRNAs), and natural antisense transcript siRNAs (nat-siRNAs) (Baulcombe, 2004; Axtell, 2013;
65 Borges *et al.*, 2015). During ra-siRNA biogenesis, the plant specific DNA-dependent RNA
66 polymerase IV (Pol IV) uses repeated DNAs as templates to produce RNA precursors, which are
67 then converted to dsRNAs by RDR2. The resulting dsRNAs are mainly processed by DCL3, a
68 homolog of DCL1, to generate ~24 nt ra-siRNAs (Law & Jacobsen, 2010; Castel & Martienssen,
69 2013; Matzke & Mosher, 2014; Xie & Yu, 2015). Pha-siRNAs including trans-acting siRNAs
70 (ta-siRNAs) are secondary siRNAs. Their production begins with miRNA-mediated cleavage of
71 target transcripts (Fei *et al.*, 2013). RDR6 then uses the resulted cleavage products as templates
72 to synthesize dsRNAs, which are processed by DCL4 to generate ta-siRNAs (Allen *et al.*, 2005;
73 Yoshikawa *et al.*, 2005; Axtell *et al.*, 2006). Compared with ra-siRNAs and pha-siRNAs, the
74 precursor dsRNAs of nat-siRNAs are formed by independently transcribed complementary
75 RNAs (Zhang *et al.*, 2013). Besides endogenous siRNAs, plants also generate exogenous
76 siRNAs from transgenes such as sense transgenes (s-siRNAs) or transgenes of inverted repeats
77 (IR-siRNAs) (Vaucheret & Fagard, 2001; Ossowski *et al.*, 2008).

78
79 In plants, the DNA-dependent RNA Polymerase II (Pol II) transcribes most miRNA-coding
80 genes (MIRs) to pri-miRNAs, with assistance from the Mediator complex (Kim *et al.*, 2011), the
81 Elongator complex (Fang *et al.*, 2015), Negative on TATA less 2 (NOT2) (Wang *et al.*, 2013)
82 and CELL DIVISION CYCLE 5 (CDC5) (Zhang *et al.*, 2013). Following transcription, the
83 RNase III enzyme DICER-LIKE1 (DCL1) cleaves pri-miRNAs at least two times to release a
84 miRNA/miRNA* (Passenger strand) in the nucleus (Baulcombe, 2004). Many DCL1-associated
85 proteins are also required for pri-miRNA processing, such as HYL1 (a double stranded RNA-
86 binding protein) (Dong *et al.*, 2008), SERRATE (SE, a Zinc-finger protein) (Grigg *et al.*, 2005),
87 TOUGH (TGH, an RNA-binding protein) (Ren *et al.*, 2012), the Elongator complex (Fang *et al.*,
88 2015), NOT2 (Wang *et al.*, 2013), CDC5 (Zhang *et al.*, 2013), PLEIOTROPIC REGULATORY
89 LOCUS 1 (PRL1) (Zhang *et al.*, 2014), MAC3 (Li *et al.*, 2018) and CBP20/80 (two cap-binding

90 proteins) (Gregory *et al.*, 2008; Laubinger *et al.*, 2008). Moreover, some proteins may also
91 regulate the accumulation of miRNAs by modulating the levels or activities of the DCL1
92 complex or promoting the recruitment of pri-miRNAs to the DCL1 complex. Examples of such
93 proteins include MODIFIER OF SNC1, 2 (MOS2, an RNA-binding protein) (Wu *et al.*, 2013),
94 the ribosome protein STV1 (Li *et al.*, 2017), the proline-rich SICKLE (SIC) (Zhan *et al.*, 2012),
95 RECEPTOR FOR ACTIVATED C KINASE 1 (RACK1) (Speth *et al.*, 2013), the pre-mRNA
96 processing factor 6 homolog STABILIZED1 (STA1) (Ben Chaabane *et al.*, 2013),
97 REGULATOR OF CBF GENE EXPRESSION 3 (RCF3, also known as HOS5 and SHI1) (Chen
98 *et al.*, 2015; Karlsson *et al.*, 2015) and the glycine-rich RNA-binding protein GRP7 (Koster *et al.*,
99 2014).

100

101 DAWDLE (DDL) is a conserved forkhead-associated domain (FHA)-containing protein that is
102 required for proper development and immune responses (Morris *et al.*, 2006; Feng *et al.*, 2016).
103 Recently, DDL was shown to regulate the biogenesis of several miRNAs and ra-siRNAs (Yu *et*
104 *al.*, 2008). However, its global effect on miRNA accumulation still is not known. Furthermore,
105 the effect of DDL on transgene-induced gene silencing is not defined. In addition, the impact of
106 DDL on the precision of miRNA processing is unknown. Moreover, DDL interacts with DCL1
107 through its FHA domain and stabilizes pri-miRNAs (Machida & Yuan, 2013), yet the biological
108 significance of this interaction in miRNA biogenesis remains elusive.

109

110 Here we report that DDL globally influences the accumulation of miRNAs and ra-siRNAs and is
111 also required for the biogenesis of S-siRNAs and IR-siRNAs. We further show that a mutation
112 abolishing the DDL-DCL1 interaction disrupts pri-miRNA processing, demonstrating that the
113 DDL-DCL1 interaction is required for miRNA biogenesis. Interestingly, this mutation also
114 disrupts the interaction of DDL with DCL3 and impairs the activity of DCL3. These results
115 suggest that DDL may participate in small RNA biogenesis by modulating the activity of DCLs.

116

117 **Results**

118

119 **DDL globally affects the accumulation of miRNAs and siRNAs.**

120 To determine the global effect of DDL on the accumulation of miRNAs and siRNAs, we
121 compared the small RNA profile in *ddl-1* with that in Ws (wild type, WT). Small RNA libraries
122 prepared from inflorescences of *ddl-1* and Ws were subjected to Illumina deep sequencing
123 analyses. Many miRNAs were reduced in abundance in *ddl-1* relative to Ws in two biological
124 replicates (Figure 1A). RNA blot analyses of several miRNAs (miR164, miR162, miR163,
125 miR158, miR159/miR319, miR173 and miR390) further validated the deep-sequencing results
126 (Figure 1B), suggesting that DDL is required for miRNA biogenesis. We also determined the
127 effect of DDL on precision of pri-miRNA processing. If precisely processed, miRNAs or
128 miRNA*s should fall within ± 2 bases of the annotated mature miRNA(s) or miRNA*(s)
129 positions (Liu *et al.*, 2012). We focused our analyses on those with high readings, because
130 evaluation of miRNA precision relies on sequencing depth. We did not detect significant
131 differences of miRNA precision between Ws and *ddl-1* (DataSet S1).

132

133 Next, we analyzed the effect of DDL on siRNAs at global levels as described (Shahid & Axtell,
134 2014). We obtained short read counts to various siRNA loci using the software tool ShortStack,
135 normalized reading numbers at various loci to those of miR163, whose abundance was not
136 changed between *ddl-1* and Ws (Yu *et al.*, 2008), and compared the abundance of siRNAs in *ddl-1*
137 with that in Ws. The abundance of siRNAs from most loci was reduced in *ddl-1* relative to Ws
138 in two biological replicates (Figure 1A). Several siRNAs (Cluster4, TR2558, TAS3-5'D8(+),
139 TAS2-siR1511, FWA, Copia and Simple hat2) were further examined using RNA blots (Figure
140 1C). As observed in RNA-seq, the abundance of these examined siRNAs was reduced in *ddl-1*
141 compared with Ws. These results demonstrated that DDL plays essential roles in siRNA
142 accumulation. We further analyzed the abundance of siRNAs in *ddl-1* and Ws based on their
143 sizes (21-, 22- and 24-nt). The abundance of 21-, 22-, and 24-nt siRNAs was reduced in *ddl-1*
144 compared with Ws (Figure S1), suggesting that DDL may have a general role in siRNA
145 biogenesis.

146

147 **DDL is required for the accumulation of transgene-induced siRNAs.**

148 Next, we investigated if DDL also affects the production of transgene-induced siRNAs. We first
149 examined the effect of *ddl-1* on the sense transgene-induced siRNAs. *ddl-1* (from the Ws genetic
150 background) was crossed to the L1 line (Col genetic background) (Mourrain *et al.*, 2000), which

151 harbors a silenced 35S promoter-driven GUS sense transgene, and is often used as a reporter line
152 of sense transgene-induced gene silencing. To rule out the potential effect of different genetic
153 backgrounds, we generated a recombined inbred line through repeated self-crossing of DDL/*ddl*-
154 *1* harboring the L1 locus obtained from the original cross for five generations. In the sixth
155 generation, we obtained wild-type (*DDL*⁺) and *ddl*-*1* containing the *L1* locus and examined the
156 effect of *ddl*-*1* on GUS expression. GUS histochemical staining and RNA blot analyses revealed
157 that the expression of the GUS transgene was recovered in *ddl*-*1* compared with *DDL*⁺ (Figure
158 2A and 2B). We further examined GUS-derived siRNAs (GUS-siRNAs) from *DDL*⁺ and *ddl*-*1*
159 using RNA blots. The accumulation of GUS-siRNAs was reduced in *ddl*-*1* relative to *DDL*⁺
160 (Figure 2C). These results demonstrate that DDL is required for sense transgene-induced siRNA
161 silencing.

162

163 Then we crossed *ddl*-*1* to the *API-IR* line (Ler background) (Chuang & Meyerowitz, 2000), in
164 which the expression of an inverted repeat transgene produces siRNAs targeting the AP1 gene
165 that encodes a transcription factor controlling flower development, resulting in AP1 silencing.
166 The resulting DDL/*ddl*-*1* containing the *API-IR* locus was self-crossed for five generations to
167 produce a recombined inbred line. In the sixth generation, we examined the effect of *ddl*-*1* on the
168 accumulation of AP1 siRNAs. The levels of AP1 siRNAs were reduced in *ddl*-*1* compared with
169 WT (*DDL*⁺) (Figure 2D), suggesting that DDL may be required for IR siRNA production.
170 However, the levels of AP1 mRNAs were similar in *ddl*-*1* and WT harboring the *API-IR* lines
171 (Figure 2E). It is possible that the reduction of AP1 siRNA in *ddl*-*1* may be not sufficient to
172 repress AP1 silencing. Alternatively, DDL may have additional function in promoting *API*
173 transcript levels since many FHA-containing proteins can regulate multiple biological processes
174 (Chevalier et al., 2009). The reduction of the *API* mRNA levels in *ddl*-*1* relative to WT (Figure
175 2E) strongly supports this notion.

176

177 **DDL interacts with DCL3 but not DCL4.**

178 Next, we examined how DDL affects the accumulation of various sRNAs. We have shown that
179 DDL interacts with DCL1, the major enzyme producing miRNAs. By analogy, we hypothesized
180 that DDL might interact with DCL3 that generates ra-siRNAs and DCL4 that produces ta-
181 siRNAs and transgene-induced siRNAs. To test the DDL-DCL3 interaction and to determine the

182 protein domains of DCL3 that interacts with DDL, we co-expressed N-terminal MYC-fused full-
183 length DCL3 and four DCL3 fragments (Figure 3A), namely MYC-DCL3, MYC-F1 (aa 1–350,
184 covering amino terminus to helicase domain 1), MYC-F2 (aa 351–700; helicase domain 2),
185 MYC-F3 (aa 701–980; Piwi/Argonaute/Zwille domain), and MYC-F4 (aa 971–1580) with C-
186 terminal GFP-fused DDL in *Nicotiana benthamiana*. After co-expression, anti-GFP antibodies
187 conjugated with protein G agarose beads were used to perform IP of DDL-GFP. The full-length
188 DCL3 and F3 fragment, but not other fragments of DCL3, were detected in the DDL-GFP IP
189 (Figure 3B), revealing that DDL may interact with the PAZ domain of DCL3. We also examined
190 the interaction of DDL and DCL4. However, we did not detect the DDL-DCL4 interaction using
191 co-IP (Figure S2). Bimolecular fluorescence complementation (BiFC) was performed to confirm
192 the DDL-DCL3 interaction. In this assay, DDL was fused with the N-terminal fragment of Venus
193 (DDL-nVenus) and DCL3 was fused with C-terminal fragment of cyan fluorescent protein
194 (cCFP-DCL3). The interaction between DDL and DCL3 resulted in the production of functional
195 yellow fluorescence protein (YFP) (showing in green, Figure 3C) in the leaf cells of *N.*
196 *benthamiana* co-expressing nVenus-DDL and cCFP-DCL3. In contrast, the negative control pair
197 DDL/GUS did not produce the YFP signal (Figure 3C). These results demonstrate the DDL-
198 DCL3 interaction.

199

200 **DDL is required for the optimal activity of DCL1 and DCL3.**

201 Because the reduction of various sRNAs could be caused by impaired DCL activity, we used an
202 *in vitro* pri-miRNA processing assay to evaluate the effect of DDL on DCL1 activity (Qi *et al.*,
203 2005; Ren *et al.*, 2012). We generated a [³²P]-labeled RNA fragment containing the stem-loop of
204 pri-miR162b flanked by 6-nt arms at each end (*MIR162b*) using *in vitro* transcription and
205 examined its processing in the protein extracts from inflorescences of Ws or *ddl-1*. *ddl-1* reduced
206 the production of miR162 from *MIR162b* at various time points (Figure 4A). At 80 min, the
207 amount of miR162b generated in *ddl-1* was ~60% of that produced in Ws (Figure 4B). It was
208 also known that DCL3 catalyzes the production of 24-nt siRNA in the *in vitro* dsRNA-
209 processing assay (Qi *et al.*, 2005). We adapted this assay to test the impact of DDL on DCL3
210 activity. The amount of 24 nt siRNAs generated from a radioactive labeled dsRNA (460 bp) in
211 the *ddl-1* protein extracts was lower than that in Ws (Figure 4C and 4D). Because the protein

212 levels of DCL1 and DCL3 in the protein extracts of *ddl-1* were similar to those in Ws (Figure
213 4E), these results suggest that the activity of DCL1 and DCL3 is impaired by *ddl-1*.

214

215 **The FHA domain of DDL is required for miRNA biogenesis.**

216 DDL interacts with the helicase and RNase III domains of DCL1 and the PAZ domain of DCL3.
217 Because these domains are critical for DCL1/DCL3 activity, we reasoned that DDL may
218 promote DCL1/DCL3 activity through its interaction with DCL1/DCL3. To test this hypothesis,
219 we examined a *ddl-3* allele (Narayanan *et al.*, 2014), which is in the Col genetic background and
220 carries a Glycine-to-Arginine (G222R) change at amino acid position 222 of DDL (Figure 5A).
221 This G is highly conserved both in the sequence and the crystal structure of the FHA domain
222 (Machida & Yuan, 2013). It localizes at the protein-protein interaction face of the FHA domain
223 (Figure 5A) and is required for phospho-threonine recognition (Machida & Yuan, 2013). We
224 suspected that this G222R mutation might disrupt the DDL-DCL1 interaction and thereby affect
225 miRNA biogenesis. We compared the accumulation of miRNAs in *ddl-3* with that in wild-type
226 plants (WT; Col er-105 genotype). RNA blots revealed that the abundance of examined miRNAs
227 was reduced in *ddl-3* (Figure 5B), suggesting that the G222R mutation impaired the activity of
228 DDL in miRNA biogenesis. We also expressed the *ddl-3* cDNA in *ddl-1* to examine its effect on
229 miRNA biogenesis in the Ws background. The *ddl-1* plants harboring the *ddl-3* cDNA still
230 displayed growth defects compared to Ws (Figure 5C). In agreement with this observation, the
231 levels of miRNAs in *ddl-1* expressing the *ddl-3* cDNA were much lower than those in Ws
232 (Figure 5D). These results demonstrate that the FHA domain is required for the proper function
233 of DDL in miRNA biogenesis.

234

235 **The G222R mutation disrupted the DDL-DCL1 and DDL-DCL3 interactions and the
236 activity of DCLs.**

237 We further tested if the G222R mutation disrupted the DDL-DCL1 interaction by the co-IP assay.
238 We co-expressed GFP, C-terminal GFP fused *ddl-3* (*ddl-3*-GFP) or DDL-GFP with N-terminal
239 MYC fused DCL1 (MYC-DCL1) in *N. benthamiana*. We then performed IP with anti-GFP
240 antibodies. As expected, DDL-GFP, but not GFP, co-IPed with MYC-DCL1 (Figure 6A).
241 However, MYC-DCL1 was not detected in the *ddl-3*-GFP IPs (Figure 6A). These results
242 demonstrate that the G222R mutation abolished the interaction between DDL and DCL1. We

243 also examined the *ddl-3*-DCL3 interaction by Co-IP. Compared with the DDL-DCL3 interaction,
244 a much weaker *ddl-3*-DCL3 interaction was detected (Figure 6B). These results demonstrate that
245 the FHA domain is required for the interaction of DDL with DCLs.

246 Furthermore, we tested if *ddl-3* impaired the activity of DCLs using *in vitro* processing assay.
247 We compared the processing of *MIR162b* and dsRNA in the protein extracts of *ddl-3* with that in
248 *er-105*. The generation of miR162 and siRNAs from *MIR162b* and dsRNAs, respectively, was
249 reduced in *ddl-3* (Figure 6C and 6D), demonstrating that the G222R mutation impaired the
250 activity of DCL1 and DCL3.

251

252 **Discussion**

253 In summary, we have demonstrated that DDL plays a general role in sRNA biogenesis. This is
254 evidenced by reduced accumulation of miRNAs, ta-siRNAs, ra-siRNAs and transgene-induced
255 siRNAs in *ddl-1*. DDL may have global effect on miRNA and ra-siRNA biogenesis since many
256 miRNAs and ra-siRNAs are reduced in abundance in *ddl-1*.

257

258 DDL is able to positively regulate the accumulation of miRNAs through promoting DCL1
259 activity, which is supported by the observation that *ddl-1* and *ddl-3* reduced processing of pri-
260 miRNAs. DDL likely enhances the activity of DCL1 through its interaction with DCL1 since the
261 disruption of the DDL-DCL1 interaction impairs DCL1 activity. The FHA domain of DDL is a
262 phospho-threonine-binding domain, interacting with the helicase and RNase III domains of
263 DCL1 (Machida & Yuan, 2013). Interestingly, these two domains of DCL1 contain the predicted
264 pThr+3(Ile/Val/Leu/Asp) motif (Machida & Yuan, 2013), which raises the possibility that plants
265 use phosphorylation to control DDL-DCL1 interaction and thereby modulate miRNA biogenesis.
266 Consistent with this hypothesis, DCL1 is indeed phosphorylated *in vivo* (Engelsberger & Schulze,
267 2012). Expression of *ddl-3* partially recovered miRNA levels and developmental defects of *ddl-1*
268 (Figure 5C and 5D), suggesting that DDL may have other functions in miRNA biogenesis
269 besides its effect on DCL1 activity. In fact, DDL is an RNA-binding protein and stabilizes pri-
270 miRNAs (Yu *et al.*, 2008). Based on these analyses, we propose that DDL may affect miRNA
271 biogenesis through its combined effect on DCL1 activity and pri-miRNA stability.

272

273 DDL is required for the accumulation of 21-, 22- and 24-nt siRNAs. Because DCL4, DCL2 and
274 DCL3 are responsible for the generation of 21-, 22- and 24-nt siRNAs, respectively, our results
275 suggest that DDL may affect the activity of all DCLs in *Arabidopsis*. It likely promotes ra-
276 siRNA biogenesis as a co-factor of DCLs, given the observation that DDL interacts with DCL3
277 and facilitates its activity. DDL binds the PAZ domain of DCL3. In contrast, it interacts with the
278 helicase and RNase III domains of DCL1 (Machida & Yuan, 2013). This may have arisen from a
279 different molecular structure or phosphorylation patterns as a result of different DCL proteins.
280 DDL functions in ta-siRNA biogenesis as well. Since the production of ta-siRNAs depends on
281 miRNAs, we believe that the reduced miRNA accumulation in *ddl-1* may be at least partially
282 responsible for ta-siRNA biogenesis. DDL may also contribute to ta-siRNA biogenesis through
283 its interaction with DCL4. However, we did not detect the DDL-DCL4 interaction through co-IP,
284 although it is still possible that DDL transiently or weakly interacts with DCL4. Besides
285 endogenous sRNAs, the accumulation of transgene-induced siRNAs is also reduced in *ddl-1*.
286 Given the fact that multiple DCLs are responsible for the production of transgene-induced
287 siRNAs, it is reasonable to speculate that DDL may contribute to the biogenesis of transgene-
288 induced siRNA through its interaction of different DCLs. Alternatively, DDL may bind and
289 stabilize the precursors of transgene-induced siRNAs, and thereby contribute to the accumulation
290 of transgene-induced siRNAs.

291 **Materials and Methods**

292 **Plant Materials**

293 The *ddl-1* (CS6932) mutant is in the Ws genetic background. An L1 line (Mourrain *et al.*, 2000)
294 and AP1-IR line (Chuang & Meyerowitz, 2000) were crossed to *ddl-1*. In the F2 generation, L1,
295 *ddl-1* and *API-IR* were identified by PCR-genotyping of *GUS*, *ddl-1* and *API-IR*, respectively.
296 The resulting *DDL/ddl-1* plants harboring *L1* or *API-IR* were self-crossed for five generations. In
297 the sixth generation, the *DDL*⁺ (wild-type) and *ddl-1* plants containing *L1* or *AP-IR* were
298 identified through PCR genotyping for *ddl-1*, *GUS* or *API-IR*, respectively. *ddl-3* that contains a
299 missense point mutation is in a Columbia er-105 background (Narayanan *et al.*, 2014).
300 Constructs harboring *DDL-GFP* and *ddl-3-GFP* were transformed into *ddl-1* or *ddl-3* for
301 complementation assay.

302

303 **Small RNA-seq and Data Analysis**

304 RNA blot analysis of small RNAs and RT-qPCR analysis of pri-miRNA transcription levels
305 were performed as described (Ren *et al.*, 2012). Small RNA libraries from inflorescences were
306 prepared and sequenced using Illumina Genome Analyzer IIx following the standard protocol.
307 Adapters from the 3' end of reads were trimmed off and trimmed reads shorter than 12
308 nucleotides or longer than 30 nucleotides were excluded from further analysis. Clean reads were
309 mapped to either the *Arabidopsis* genome (TAIR 9.0, for both miRNA and siRNA abundance) or
310 miRNA hairpin sequences (from miRBase v1.8, for miRNA imprecision) using Bowtie with up
311 to 1 mismatch (Langmead *et al.*, 2009). EdgeR with TMM normalization method was used for
312 differential analysis (Robinson *et al.*, 2010; Robinson & Oshlack, 2010). The miRNA/miRNA*
313 imprecision ratios were determined and analyzed using the same method described by Liu *et al.*
314 (Liu *et al.*, 2012). Shortstack (Shahid & Axtell, 2014) was used to find the siRNA clusters. The
315 cluster read counts are reads mapped to each cluster (+/-150bp) and normalized to counts of
316 miR163, whose abundance is not changed in *ddl-1*.

317

318 **Plasmid Construction**

319 *DDL* cDNA and *DCL3* cDNA were cloned into pSAT4-C-nVenus and pSAT4-C-cCFP,
320 respectively (Ren *et al.*, 2012). The *DDL-C-nVenus* and *DCL3-C-cCFP* fragments were then
321 released by I-SceI restriction enzyme digestion and subsequently cloned into the pPZP-ocs-bar-
322 RCS2-2 vector. The truncated *DCL3* (F1 to F4)-MYC fragments were cloned into vector
323 pGWB520. cDNAs of *DDL* and *ddl-3* were cloned into vector pMDC83 to obtain constructs
324 harboring *DDL-GFP* and *ddl-3-GFP*, respectively. The primers used for plasmid construction are
325 listed in Table S1.

326

327 **Co-Immunoprecipitation (Co-IP) assay**

328 For *DDL-DCL3* co-IP, MYC-DCL3 and truncated MYC-DCL3 (F1 to F4) were expressed in *N.*
329 *benthamiana* and protein extract from plants expressing 35S::*DDL-GFP* was incubated with
330 anti-GFP (Clontech) antibody coupled to protein G-agarose beads for 4 hours at 4 °C. After
331 washing five-times, the proteins in the immunoprecipitates were subjected to immunoblot
332 analysis using anti-GFP antibody and anti-MYC antibodies, respectively.

333

334 **Dicer Activity Assay**

335 Pri-miR162b and DsRNA were prepared by *in vitro* transcription under the presence of [α -³²P]
336 UTP. *In vitro* dicer activity assay was performed (Qi *et al.*, 2005; Ren *et al.*, 2012). Radioactive
337 signals were quantified with ImageQuant version 5.2.

338

339 **BiFC Assay**

340 Paired nVenus-DDL with cCFP-DCL3 or cCFP-GUS was co-infiltrated into *N. benthamiana*
341 leaves. After 48 hours, yellow fluorescence signals and chlorophyll autofluorescence signals
342 were excited at 488 nm and detected by confocal microscopy (Fluoview 500 workstation;
343 Olympus) with a narrow barrier filter (BA505–525 nm).

344

345 **Accession Numbers**

346 Sequence data from this article can be found in the GenBank/EMBL data libraries under
347 accession numbers GSM2809457, GSM2809458, GSM2809459 and GSM2809460.

348

349 **Supplemental Data**

350 Figure S1. Deep sequencing analysis of mature siRNAs in different size accumulation in *ddl-1*.

351 Figure S2. DDL does not interact with DCL4.

352 Table S1. DNA oligos used in this study.

353 Data Set S1 (XLS) The effect of DDL on the precision of miRNA processing.

354

355 **Acknowledgements**

356 This work was supported by Taishan Scholars (Award tsqn20161020 to S.Z), Nebraska Soybean
357 Board (Award 16R-05-3/3 #1706 to B.Y) and National Science Foundation (Awards OIA-
358 1557417 to B.Y).

359

360

361 **Figure legends**

362 **Figure 1. DDL regulates the accumulation of miRNAs and siRNAs.** **A.** Deep sequencing
363 analysis of mature miRNA and siRNA accumulation in *ddl-1*. Libraries of small RNA were
364 produced from inflorescences of *ddl-1* and Ws. Each circle represents a small RNA calculated as
365 reads per million, and a \log_2 -transformed ratio of *ddl-1*/Ws was plotted. The thick lines in the
366 middle of circles indicate median values. Rep1 and Rep2 were two biological replicates of
367 sequencing. **B.** miRNA abundance in inflorescences of *ddl-1* and Ws. **C.** siRNA abundance in
368 inflorescences of *ddl-1* and Ws. Ws: wild-type control of *ddl-1*. U6: spliceosomal RNA U6, used
369 as loading control. Small RNAs were detected by RNA blot. Radioactive signals were detected
370 with a phosphor imager and quantified with ImageQuant (v5.2). The amount of miRNA or
371 siRNA in *ddl-1* was normalized to U6 RNA and compared with that in Ws (Set as 1) to
372 determine the relative abundance of small RNAs in *ddl-1*. The number below *ddl-1* indicated the
373 relative abundance of miRNAs or siRNAs, which is the average value of three replicates. $P <$
374 0.05; For, miR159/319: upper band, miR159; lower band, miR319. The numbers represent the
375 relative abundance quantified by three replicates (T test, $P < 0.05$).

376 **Figure 2. DDL is required for transgene induced siRNA accumulation.** **A.** Histochemical
377 staining of GUS in plants containing the *L1* locus. Wild-type (DDL^+) and *ddl-1* containing the *L1*
378 locus were segregated from the sixth generation of a recombined inbred line through repeated
379 five generations of self-crossing of *DDL/ddl-1* harboring the *L1* locus. Twenty plants containing
380 *GUS* were analyzed for each genotype. **B.** *GUS* mRNA levels in DDL^+ and *ddl-1* detected by
381 RNA blot. Equal total RNAs were loaded for RNA blot. **C.** The accumulation of *GUS* siRNA in
382 DDL^+ and *ddl-1*. **D.** The accumulation of AP1 siRNAs in DDL^+ , $DDL^+/API-IR$, *ddl-1* and *ddl-*
383 *I/API-IR* plants detected by RNA blot. U6 RNA was used as loading control. **E.** *API* expression
384 levels in DDL^+ , $DDL^+/API-IR$, *ddl-1* and *ddl-1/API-IR*. DDL^+ , $DDL^+/API-IR$, *ddl-1* and *ddl-*
385 *I/API-IR* plants were segregated from a recombined inbred line that was produced by five
386 generations of repeated self-crossing of *DDL/ddl-1* containing the *API-IR* locus. Equal total
387 RNAs were loaded for the RNA blot.

388 **Figure 3. DDL interacts with DCL3.** **A.** Schematic diagram of DCL3 domains and truncated
389 DCL3 fragments used for protein interaction assay. **B.** The interaction between DDL and various
390 DCL3 fragments detected by co-immunoprecipitation (co-IP). Full-length and truncated DCL3
391 proteins fused with a MYC tag at their N-terminus were expressed in *N. benthamiana* leaves. For

392 DDL, protein extract from plants expressing *35S::DDL-GFP*. The protein pairs in the protein
393 extracts were indicated by the labels on the left side and above the picture. An anti-MYC
394 antibody was used to detect MYC fusion proteins in immunoblots. Labels on left side of picture
395 indicate proteins detected by immunoblot. Five percent input proteins were used for MYC tagged
396 proteins while twenty percent inputs were used for *DDL-GFP*. **C.** BiFc analysis of the interaction
397 DDL with DCL3. Paired of nVenus and cCFP fused proteins were co-infiltrated into *N.*
398 *benthamiana* leaves. Yellow fluorescence (green in image) signals were examined at 48 h after
399 infiltration by confocal microscopy. The red spots were autofluorescence from chlorophyll. One
400 hundred nuclei were examined randomly for each pair of proteins and one image was shown, the
401 percentage of cells with fluorescence was shown in the images. Scale bar, 20 μ m.

402 **Figure 4. *ddl-1* reduces the accumulation of miR162 and siRNA in an *in vitro* processing**
403 **assay. A.** miRNA production from pri-miR162b in the protein extracts of *ddl-1* and Ws. [32 P]-
404 labeled *MIR162b* that contains the stem-loop of pri-miR162b flanked by 6-nt arms at each end
405 was generated through *in vitro* transcription. **B.** Quantification of miRNAs generated from pri-
406 miR162b in *ddl-1* compared to those in Ws at 40 min, 80 min and 120 min. **C.** siRNA production
407 from dsRNAs in the protein extracts isolated from inflorescences of *ddl-1* and Ws. dsRNAs were
408 synthesized through *in vitro* transcription of a DNA fragment (5' portion of *UBQ5* gene, ~460 bp)
409 under the presence of [α - 32 P] UTP. **D.** Quantification of siRNAs produced from dsRNAs in *ddl-1*
410 compared to those in Ws at 40 min, 80 min and 120 min. The amounts of miRNAs or siRNAs
411 produced at 40 min from Ws were set as 1, and means \pm SD were calculated from three
412 biological replicates. **E.** The protein levels of DCL1 and DCL3 in protein extracts of Ws and *ddl-1*
413 detected by immunoblot. Hsc70 was used as loading control.

414 **Figure 5. The FHA domain of DDL is required for miRNA biogenesis. A.** Schematic diagram
415 of DDL protein domains and the G222R mutation of *ddl-3*. Arg rich region: Arginine rich
416 domain, NLS: Nuclear Localization Signal, FHA: Forkhead Associated Domain. **B.** miRNA and
417 siRNA abundance in inflorescences of Ws, *ddl-1*, *er105* and *ddl-3* detected by RNA blotting. **C.**
418 The phenotypes of *ddl-1* harboring the *DDL-GFP* or the *ddl-3-GFP* transgenes. **D.** miRNA
419 abundance in various genotypes detected by RNA blotting. The radioactive signals were detected
420 with a phosphor imager and quantified with ImageQuant (v5.2). The amount of a small RNA
421 was normalized to U6 RNA and compared with Ws. The numbers represent the relative

422 abundance quantified in three replicates (T test, $P < 0.05$). Ws: background control of *ddl-1*; er-
423 105: control of *ddl-3*.

424

425 **Figure 6. The G222R mutation disrupts the DDL-DCL1 and DDL-DCL3 interactions and**
426 **the activity of DCLs. A and B.** Interactions of *ddl-3* with DCL1 (A) and DCL3 (B) examined
427 by co-IP. GFP, *ddl-3* fused with GFP at its C-terminal (*ddl-3*-GFP) or DDL-GFP were co-
428 expressed with N-terminal MYC fused DCL1 (MYC-DCL1) or DCL3 (MYC-DCL3) in *N.*
429 *benthamiana*. Anti-GFP antibodies were used to perform IP and anti-MYC antibody was used to
430 detect MYC fusion proteins in immunoblots. Five percent input proteins were used for
431 immunoblots. **C and D.** *MIR162b* (C) and dsRNA (D) processing by protein extracts of *ddl-3* and
432 er-105, respectively. [32 P]-labeled *MIR162b* that contains the stem-loop of pri-miR162b flanked
433 by 6-nt arms at each end was generated through *in vitro* transcription. dsRNAs were synthesized
434 through *in vitro* transcription of a DNA fragment (5' portion of *UBQ5* gene, ~460 bp) under the
435 presence of [α - 32 P] UTP. Proteins were isolated from inflorescences of *ddl-3* or er-105. The *in*
436 *vitro* processing reactions were stopped at 80 min and RNAs were extracted for gel running.
437 Radioactive signals were quantified with ImageQuant (v5.2).

438

439 **References:**

440 **Allen E, Xie Z, Gustafson AM, Carrington JC. 2005.** microRNA-directed phasing during
441 trans-acting siRNA biogenesis in plants. *Cell* **121**(2): 207-221.

442 **Axtell MJ. 2013.** Classification and comparison of small RNAs from plants. *Annu Rev Plant*
443 *Biol* **64**: 137-159.

444 **Axtell MJ, Jan C, Rajagopalan R, Bartel DP. 2006.** A two-hit trigger for siRNA biogenesis in
445 plants. *Cell* **127**(3): 565-577.

446 **Baulcombe D. 2004.** RNA silencing in plants. *Nature* **431**(7006): 356-363.

447 **Ben Chaabane S, Liu R, Chinnusamy V, Kwon Y, Park JH, Kim SY, Zhu JK, Yang SW,**
448 **Lee BH. 2013.** STA1, an *Arabidopsis* pre-mRNA processing factor 6 homolog, is a new
449 player involved in miRNA biogenesis. *Nucleic Acids Res* **41**(3): 1984-1997.

450 **Borges F, Martienssen RA. 2015.** The expanding world of small RNAs in plants. *Nat Rev Mol*
451 *Cell Biol* **16**(12): 727-741.

452 **Castel SE, Martienssen RA. 2013.** RNA interference in the nucleus: roles for small RNAs in
453 transcription, epigenetics and beyond. *Nat Rev Genet* **14**(2): 100-112.

454 **Chen T, Cui P, Xiong L. 2015.** The RNA-binding protein HOS5 and serine/arginine-rich
455 proteins RS40 and RS41 participate in miRNA biogenesis in *Arabidopsis*. *Nucleic Acids*
456 *Res* **43**(17): 8283-8298.

457 **Chevalier D, Morris ER, Walker JC** (2009) 14-3-3 and FHA domains mediate phosphoprotein
458 interactions. *Annu Rev Plant Biol* **60**: 67-91

459 **Chuang CF, Meyerowitz EM.** **2000.** Specific and heritable genetic interference by double-
460 stranded RNA in *Arabidopsis thaliana*. *Proc Natl Acad Sci U S A* **97**(9): 4985-4990.

461 **Dong Z, Han MH, Fedoroff N.** **2008.** The RNA-binding proteins HYL1 and SE promote
462 accurate in vitro processing of pri-miRNA by DCL1. *Proc Natl Acad Sci U S A* **105**(29):
463 9970-9975.

464 **Engelsberger WR, Schulze WX.** **2012.** Nitrate and ammonium lead to distinct global dynamic
465 phosphorylation patterns when resupplied to nitrogen-starved *Arabidopsis* seedlings.
466 *Plant J* **69**(6): 978-995.

467 **Fang X, Cui Y, Li Y, Qi Y.** **2015.** Transcription and processing of primary microRNAs are
468 coupled by Elongator complex in *Arabidopsis*. *Nat Plants* **1**: 15075.

469 **Fei Q, Xia R, Meyers BC** (2013) Phased, secondary, small interfering RNAs in
470 posttranscriptional regulatory networks. *Plant Cell* **25**: 2400-2415

471 **Feng B, Ma S, Chen S, Zhu N, Zhang S, Yu B, Yu Y, Le B, Chen X, Dinesh-Kumar SP,**
472 **Shan L, He P.** **2016.** PARylation of the forkhead-associated domain protein DAWDLE
473 regulates plant immunity. *EMBO Rep* **17**(12): 1799-1813.

474 **Gregory BD, O'Malley RC, Lister R, Urich MA, Tonti-Filippini J, Chen H, Millar AH,**
475 **Ecker JR.** **2008.** A link between RNA metabolism and silencing affecting *Arabidopsis*
476 development. *Dev Cell* **14**(6): 854-866.

477 **Grigg SP, Canales C, Hay A, Tsiantis M.** **2005.** SERRATE coordinates shoot meristem
478 function and leaf axial patterning in *Arabidopsis*. *Nature* **437**(7061): 1022-1026.

479 **Karlsson P, Christie MD, Seymour DK, Wang H, Wang X, Hagmann J, Kulcheski F,**
480 **Manavella PA.** **2015.** KH domain protein RCF3 is a tissue-biased regulator of the plant
481 miRNA biogenesis cofactor HYL1. *Proc Natl Acad Sci U S A* **112**(45): 14096-14101.

482 **Kim YJ, Zheng B, Yu Y, Won SY, Mo B, Chen X.** **2011.** The role of Mediator in small and
483 long noncoding RNA production in *Arabidopsis thaliana*. *EMBO J* **30**(5): 814-822.

484 **Koster T, Meyer K, Weinholdt C, Smith LM, Lummer M, Speth C, Grosse I, Weigel D,**
485 **Staiger D.** **2014.** Regulation of pri-miRNA processing by the hnRNP-like protein
486 AtGRP7 in *Arabidopsis*. *Nucleic Acids Res* **42**(15): 9925-9936.

487 **Langmead B, Trapnell C, Pop M, Salzberg SL.** **2009.** Ultrafast and memory-efficient
488 alignment of short DNA sequences to the human genome. *Genome Biol* **10**(3): R25.

489 **Laubinger S, Sachsenberg T, Zeller G, Busch W, Lohmann JU, Ratsch G, Weigel D.** **2008.**
490 Dual roles of the nuclear cap-binding complex and SERRATE in pre-mRNA splicing and
491 microRNA processing in *Arabidopsis thaliana*. *Proc Natl Acad Sci U S A* **105**(25): 8795-
492 8800.

493 **Law JA, Jacobsen SE.** **2010.** Establishing, maintaining and modifying DNA methylation
494 patterns in plants and animals. *Nat Rev Genet* **11**(3): 204-220.

495 **Li S, Liu K, Zhang S, Wang X, Rogers K, Ren G, Zhang C, Yu B.** **2017.** STV1, a ribosomal
496 protein, binds primary microRNA transcripts to promote their interaction with the
497 processing complex in *Arabidopsis*. *Proc Natl Acad Sci U S A* **114**(6): 1424-1429.

498 **Li S, Liu K, Zhou B, Li M, Zhang S, Zeng L, Zhang C, Yu B** (2018) MAC3A and MAC3B,
499 Two Core Subunits of the MOS4-Associated Complex, Positively Influence miRNA
500 Biogenesis. *Plant Cell* **30**: 481-494

501 **Liu C, Axtell MJ, Fedoroff NV. 2012.** The helicase and RNaseIIIa domains of Arabidopsis
502 Dicer-Like1 modulate catalytic parameters during microRNA biogenesis. *Plant Physiol*
503 **159**(2): 748-758.

504 **Machida S, Yuan YA. 2013.** Crystal structure of Arabidopsis thaliana Dawdle forkhead-
505 associated domain reveals a conserved phospho-threonine recognition cleft for dicer-like
506 1 binding. *Mol Plant* **6**(4): 1290-1300.

507 **Matzke MA, Mosher RA. 2014.** RNA-directed DNA methylation: an epigenetic pathway of
508 increasing complexity. *Nat Rev Genet* **15**(6): 394-408.

509 **Morris ER, Chevalier D, Walker JC. 2006.** DAWDLE, a forkhead-associated domain gene,
510 regulates multiple aspects of plant development. *Plant Physiol* **141**(3): 932-941.

511 **Mourrain P, Beclin C, Elmayan T, Feuerbach F, Godon C, Morel JB, Jouette D, Lacombe
512 AM, Nikic S, Picault N, Remoue K, Sanial M, Vo TA, Vaucheret H. 2000.** Arabidopsis SGS2 and SGS3 genes are required for posttranscriptional gene silencing
513 and natural virus resistance. *Cell* **101**(5): 533-542.

514 **Narayanan L, Mukherjee D, Zhang S, Yu B, Chevalier D. 2014.** Mutational analyses of a
515 ForkHead Associated domain protein, DAWDLE, in Arabidopsis thaliana. *American
516 Journal of Plant Sciences* **5**: 2811-2822.

517 **Ossowski S, Schwab R, Weigel D. 2008.** Gene silencing in plants using artificial microRNAs
518 and other small RNAs. *Plant J* **53**(4): 674-690.

519 **Qi Y, Denli AM, Hannon GJ. 2005.** Biochemical specialization within Arabidopsis RNA
520 silencing pathways. *Mol Cell* **19**(3): 421-428.

521 **Ren G, Xie M, Dou Y, Zhang S, Zhang C, Yu B. 2012.** Regulation of miRNA abundance by
522 RNA binding protein TOUGH in Arabidopsis. *Proc Natl Acad Sci U S A* **109**(31): 12817-
523 12821.

524 **Robinson MD, McCarthy DJ, Smyth GK. 2010.** edgeR: a Bioconductor package for
525 differential expression analysis of digital gene expression data. *Bioinformatics* **26**(1):
526 139-140.

527 **Robinson MD, Oshlack A. 2010.** A scaling normalization method for differential expression
528 analysis of RNA-seq data. *Genome Biol* **11**(3): R25.

529 **Shahid S, Axtell MJ. 2014.** Identification and annotation of small RNA genes using ShortStack.
530 *Methods* **67**(1): 20-27.

531 **Speth C, Willing EM, Rausch S, Schneeberger K, Laubinger S. 2013.** RACK1 scaffold
532 proteins influence miRNA abundance in Arabidopsis. *Plant J* **76**(3): 433-445.

533 **Vaucheret H. 2008.** Plant ARGONAUTES. *Trends Plant Sci* **13**(7): 350-358.

534 **Vaucheret H, Fagard M. 2001.** Transcriptional gene silencing in plants: targets, inducers and
535 regulators. *Trends Genet* **17**(1): 29-35.

536 **Voinnet O. 2009.** Origin, biogenesis, and activity of plant microRNAs. *Cell* **136**(4): 669-687.

537 **Wang L, Song X, Gu L, Li X, Cao S, Chu C, Cui X, Chen X, Cao X. 2013.** NOT2 proteins
538 promote polymerase II-dependent transcription and interact with multiple MicroRNA
539 biogenesis factors in Arabidopsis. *Plant Cell* **25**(2): 715-727.

540 **Wu X, Shi Y, Li J, Xu L, Fang Y, Li X, Qi Y. 2013.** A role for the RNA-binding protein
541 MOS2 in microRNA maturation in Arabidopsis. *Cell Res* **23**(5): 645-657.

542 **Xie M, Yu B. 2015.** siRNA-directed DNA Methylation in Plants. *Curr Genomics* **16**(1): 23-31.

543 **Yoshikawa M, Peragine A, Park MY, Poethig RS. 2005.** A pathway for the biogenesis of
544 trans-acting siRNAs in Arabidopsis. *Genes Dev* **19**(18): 2164-2175.

546 **Yu B, Bi L, Zheng BL, Ji LJ, Chevalier D, Agarwal M, Ramachandran V, Li WX,**
547 **Lagrange T, Walker JC, Chen XM.** 2008. The FHA domain proteins DAWDLE in
548 Arabidopsis and SNIP1 in humans act in small RNA biogenesis. *Proc Natl Acad Sci U S*
549 *A* **105**(29): 10073-10078.

550 **Zhang X, Lii Y, Wu Z, Polishko A, Zhang H, Chinnusamy V, Lonardi S, Zhu JK, Liu R,**
551 **Jin H** (2013) Mechanisms of small RNA generation from cis-NATs in response to
552 environmental and developmental cues. *Mol Plant* **6**: 704-715

553

554 **Zhan X, Wang B, Li H, Liu R, Kalia RK, Zhu JK, Chinnusamy V.** 2012. Arabidopsis
555 proline-rich protein important for development and abiotic stress tolerance is involved in
556 microRNA biogenesis. *Proc Natl Acad Sci U S A* **109**(44): 18198-18203.

557 **Zhang S, Liu Y, Yu B.** 2014. PRL1, an RNA-binding protein, positively regulates the
558 accumulation of miRNAs and siRNAs in Arabidopsis. *PLoS Genet* **10**(12): e1004841.

559 **Zhang S, Liu Y, Yu B.** 2015. New insights into pri-miRNA processing and accumulation in
560 plants. *Wiley Interdiscip Rev RNA* **6**(5): 533-545.

561 **Zhang S, Xie M, Ren G, Yu B.** 2013. CDC5, a DNA binding protein, positively regulates
562 posttranscriptional processing and/or transcription of primary microRNA transcripts.
563 *Proc Natl Acad Sci U S A* **110**(43): 17588-17593.

564

565

566

567

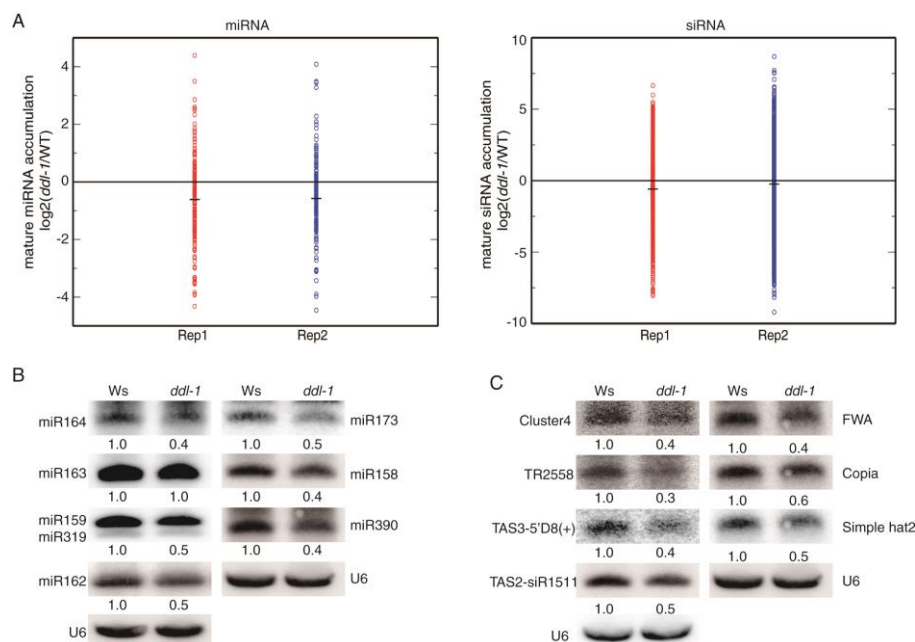


Figure 1. DDL regulates the accumulation of miRNAs and siRNAs. **A.** Deep sequencing analysis of mature miRNA and siRNA accumulation in *ddl-1*. Libraries of small RNA were produced from inflorescences of *ddl-1* and Ws. Each circle represents a small RNA calculated as reads per million, and a \log_2 -transformed ratio of *ddl-1*/Ws was plotted. The thick lines in the middle of circles indicate median values. Rep1 and Rep2 were two biological replicates of sequencing. **B.** miRNA abundance in inflorescences of *ddl-1* and Ws. **C.** siRNA abundance in inflorescences of *ddl-1* and Ws. Ws: wild-type control of *ddl-1*. U6: spliceosomal RNA U6, used as loading control. Small RNAs were detected by RNA blot. Radioactive signals were detected with a phosphor imager and quantified with ImageQuant (v5.2). The amount of miRNA or siRNA in *ddl-1* was normalized to U6 RNA and compared with that in Ws (Set as 1) to determine the relative abundance of small RNAs in *ddl-1*. The number below *ddl-1* indicated the relative abundance of miRNAs or siRNAs, which is the average value of three replicates. $P < 0.05$; For, miR159/319: upper band, miR159; lower band, miR319. The numbers represent the relative abundance quantified by three replicates (T test, $P < 0.05$).

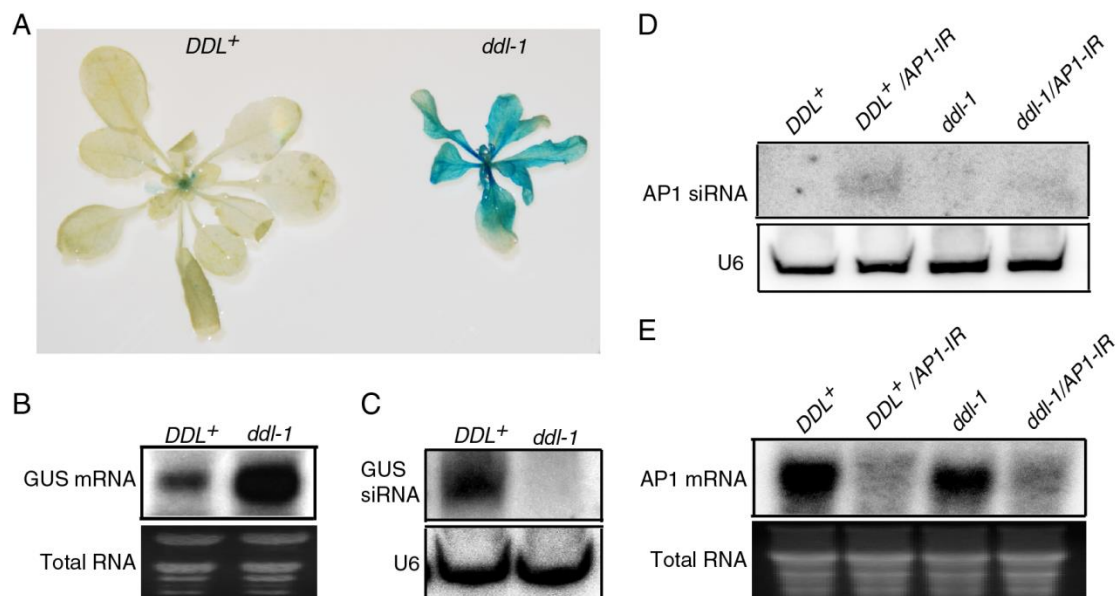


Figure 2. *DDL* is required for transgene induced siRNA accumulation. A. Histochemical staining of GUS in plants containing the *L1* locus. Wild-type (*DDL*⁺) and *ddl*-1 containing the *L1* locus were segregated from the sixth generation of a recombined inbred line through repeated five generations of self-crossing of *DDL/ddl*-1 harboring the *L1* locus. Twenty plants containing *GUS* were analyzed for each genotype. **B.** *GUS* mRNA levels in *DDL*⁺ and *ddl*-1 detected by RNA blot. Equal total RNAs were loaded for RNA blot. **C.** The accumulation of *GUS* siRNA in *DDL*⁺ and *ddl*-1. **D.** The accumulation of AP1 siRNAs in *DDL*⁺, *DDL*⁺/AP1-IR, *ddl*-1 and *ddl*-1/AP1-IR plants detected by RNA blot. U6 RNA was used as loading control. **E.** *AP1* expression levels in *DDL*⁺, *DDL*⁺/AP1-IR, *ddl*-1 and *ddl*-1/AP1-IR. *DDL*⁺, *DDL*⁺/AP1-IR, *ddl*-1 and *ddl*-1/AP1-IR plants were segregated from a recombined inbred line that was produced by five generations of repeated self-crossing of *DDL/ddl*-1 containing the *AP1-IR* locus. Equal total RNAs were loaded for the RNA blot.

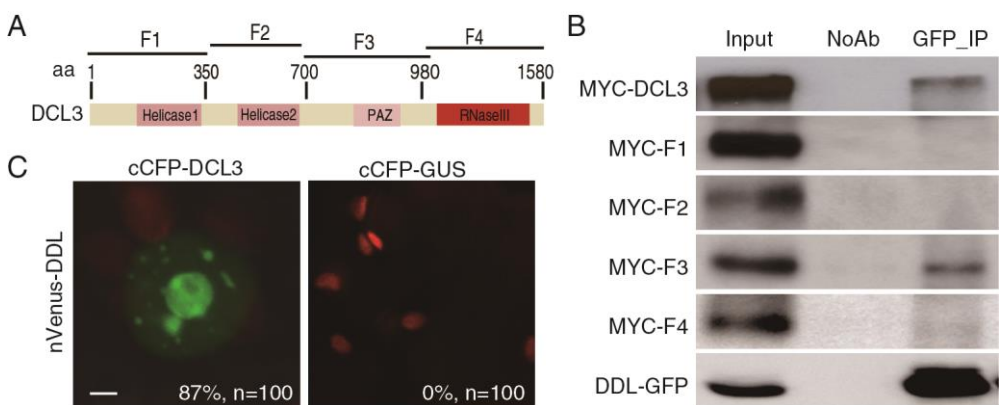


Figure 3. DDL interacts with DCL3. **A.** Schematic diagram of DCL3 domains and truncated DCL3 fragments used for protein interaction assay. **B.** The interaction between DDL and various DCL3 fragments detected by co-immunoprecipitation (co-IP). Full-length and truncated DCL3 proteins fused with a MYC tag at their N-terminus were expressed in *N. benthamiana* leaves. For DDL, protein extract from plants expressing 35S::DDL-GFP. The protein pairs in the protein extracts were indicated by the labels on the left side and above the picture. An anti-MYC antibody was used to detect MYC fusion proteins in immunoblots. Labels on left side of picture indicate proteins detected by immunoblot. Five percent input proteins were used for MYC tagged proteins while twenty percent inputs were used for DDL-GFP. **C.** BiFc analysis of the interaction DDL with DCL3. Paired of nVenus and cCFP fused proteins were co-infiltrated into *N. benthamiana* leaves. Yellow fluorescence (green in image) signals were examined at 48 h after infiltration by confocal microscopy. The red spots were autofluorescence from chlorophyll. One hundred nuclei were examined randomly for each pair of proteins and one image was shown, the percentage of cells with fluorescence was shown in the images. Scale bar, 20 μ m.

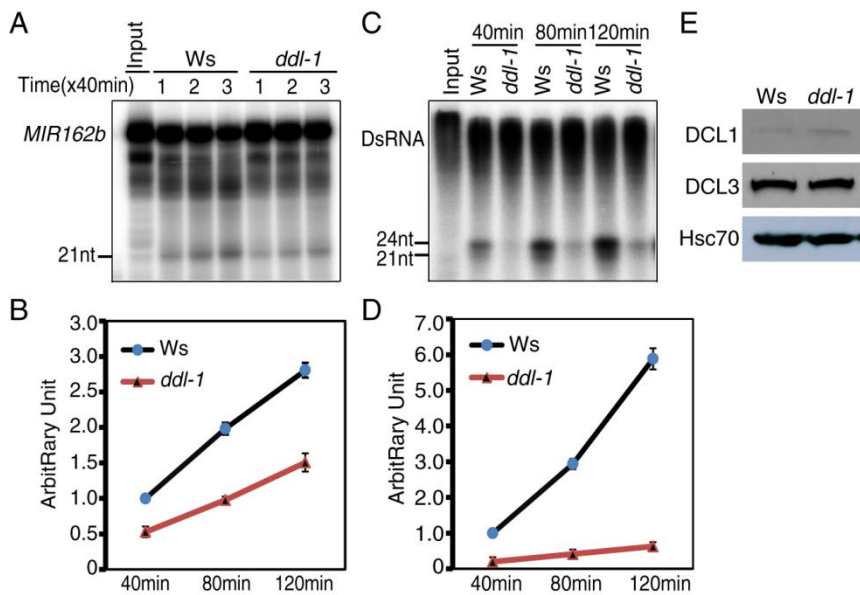


Figure 4. *ddl-1* reduces the accumulation of miR162 and siRNA in an *in vitro* processing assay. A. miRNA production from pri-miR162b in the protein extracts of *ddl-1* and Ws. [32 P]-labeled *MIR162b* that contains the stem-loop of pri-miR162b flanked by 6-nt arms at each end was generated through *in vitro* transcription. **B.** Quantification of miRNAs generated from pri-miR162b in *ddl-1* compared to those in Ws at 40 min, 80 min and 120 min. **C.** siRNA production from dsRNAs in the protein extracts isolated from inflorescences of *ddl-1* and Ws. dsRNAs were synthesized through *in vitro* transcription of a DNA fragment (5' portion of *UBQ5* gene, ~460 bp) under the presence of [α - 32 P] UTP. **D.** Quantification of siRNAs produced from dsRNAs in *ddl-1* compared to those in Ws at 40 min, 80 min and 120 min. The amounts of miRNAs or siRNAs produced at 40 min from Ws were set as 1, and means \pm SD were calculated from three biological replicates. **E.** The protein levels of DCL1 and DCL3 in protein extracts of Ws and *ddl-1* detected by immunoblot. Hsc70 was used as loading control.

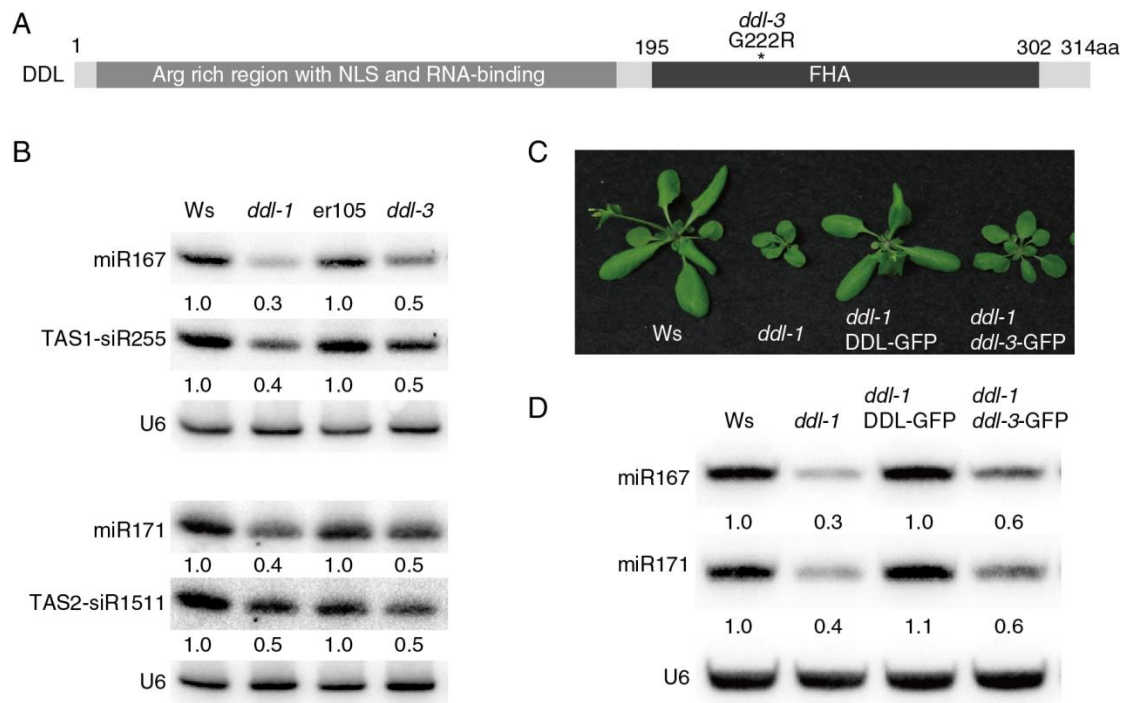


Figure 5. The FHA domain of DDL is required for miRNA biogenesis. A. Schematic diagram of DDL protein domains and the G222R mutation of *ddl-3*. Arg rich region: Arginine rich domain, NLS: Nuclear Localization Signal, FHA: Forkhead Associated Domain. **B.** miRNA and siRNA abundance in inflorescences of Ws, *ddl-1*, er105 and *ddl-3* detected by RNA blotting. **C.** The phenotypes of *ddl-1* harboring the *DDL-GFP* or the *ddl-3-GFP* transgenes. **D.** miRNA abundance in various genotypes detected by RNA blotting. The radioactive signals were detected with a phosphor imager and quantified with ImageQuant (v5.2). The amount of a small RNA was normalized to U6 RNA and compared with Ws. The numbers represent the relative abundance quantified in three replicates (T test, P < 0.05). Ws: background control of *ddl-1*; er-105: control of *ddl-3*.

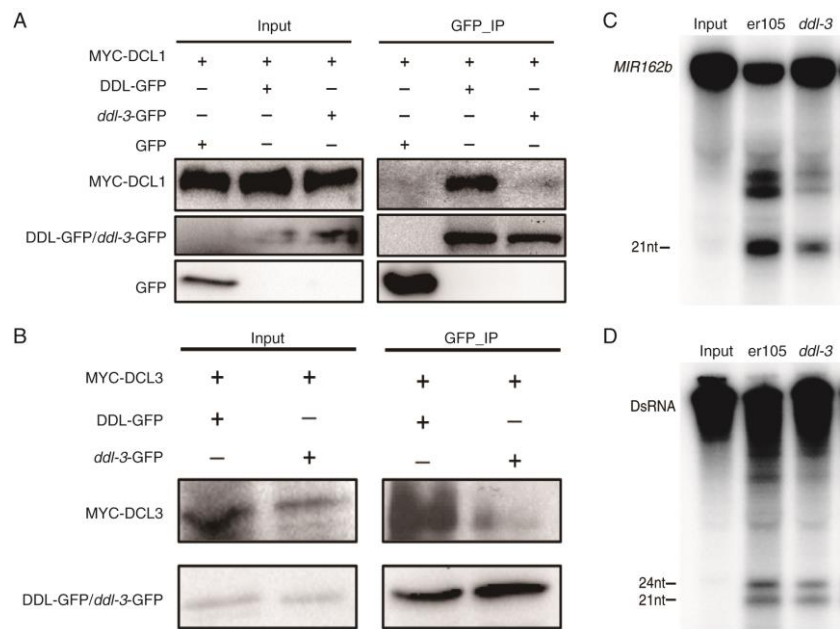


Figure 6. The G222R mutation disrupts the DDL-DCL1 and DDL-DCL3 interactions and the activity of DCLs. **A and B.** Interactions of *ddl-3* with DCL1 (A) and DCL3 (B) examined by co-IP. GFP, *ddl-3* fused with GFP at its C-terminal (*ddl-3*-GFP) or DDL-GFP were co-expressed with N-terminal MYC fused DCL1 (MYC-DCL1) or DCL3 (MYC-DCL3) in *N. benthamiana*. Anti-GFP antibodies were used to perform IP and anti-MYC antibody was used to detect MYC fusion proteins in immunoblots. Five percent input proteins were used for immunoblots. **C and D.** *MIR162b* (C) and dsRNA (D) processing by protein extracts of *ddl-3* and *er-105*, respectively. [³²P]-labeled *MIR162b* that contains the stem-loop of pri-miR162b flanked by 6-nt arms at each end was generated through *in vitro* transcription. dsRNAs were synthesized through *in vitro* transcription of a DNA fragment (5' portion of *UBQ5* gene, ~460 bp) under the presence of [α -³²P] UTP. Proteins were isolated from inflorescences of *ddl-3* or *er-105*. The *in vitro* processing reactions were stopped at 80 min and RNAs were extracted for gel running. Radioactive signals were quantified with ImageQuant (v5.2).

Parsed Citations

Allen E, Xie Z, Gustafson AM, Carrington JC. 2005. microRNA-directed phasing during trans-acting siRNA biogenesis in plants. *Cell* 121(2): 207-221.

Pubmed: [Author and Title](#)

CrossRef: [Author and Title](#)

Google Scholar: [Author Only Title Only Author and Title](#)

Axtell MJ. 2013. Classification and comparison of small RNAs from plants. *Annu Rev Plant Biol* 64: 137-159.

Pubmed: [Author and Title](#)

CrossRef: [Author and Title](#)

Google Scholar: [Author Only Title Only Author and Title](#)

Axtell MJ, Jan C, Rajagopalan R, Bartel DP. 2006. A two-hit trigger for siRNA biogenesis in plants. *Cell* 127(3): 565-577.

Pubmed: [Author and Title](#)

CrossRef: [Author and Title](#)

Google Scholar: [Author Only Title Only Author and Title](#)

Baulcombe D. 2004. RNA silencing in plants. *Nature* 431(7006): 356-363.

Ben Chaabane S, Liu R, Chinnusamy V, Kwon Y, Park JH, Kim SY, Zhu JK, Yang SW, Lee BH. 2013. STA1, an *Arabidopsis* pre-mRNA processing factor 6 homolog, is a new player involved in miRNA biogenesis. *Nucleic Acids Res* 41(3): 1984-1997.

Pubmed: [Author and Title](#)

CrossRef: [Author and Title](#)

Google Scholar: [Author Only Title Only Author and Title](#)

Borges F, Martienssen RA. 2015. The expanding world of small RNAs in plants. *Nat Rev Mol*

Pubmed: [Author and Title](#)

CrossRef: [Author and Title](#)

Google Scholar: [Author Only Title Only Author and Title](#)

Cell Biol 16(12): 727-741.

Castel SE, Martienssen RA. 2013. RNA interference in the nucleus: roles for small RNAs in transcription, epigenetics and beyond. *Nat Rev Genet* 14(2): 100-112.

Pubmed: [Author and Title](#)

CrossRef: [Author and Title](#)

Google Scholar: [Author Only Title Only Author and Title](#)

Chen T, Cui P, Xiong L. 2015. The RNA-binding protein HOS5 and serine/arginine-rich proteins RS40 and RS41 participate in miRNA biogenesis in *Arabidopsis*. *Nucleic Acids Res* 43(17): 8283-8298.

Pubmed: [Author and Title](#)

CrossRef: [Author and Title](#)

Google Scholar: [Author Only Title Only Author and Title](#)

Chevalier D, Morris ER, Walker JC (2009) 14-3-3 and FHA domains mediate phosphoprotein interactions. *Annu Rev Plant Biol* 60: 67-91

Pubmed: [Author and Title](#)

CrossRef: [Author and Title](#)

Google Scholar: [Author Only Title Only Author and Title](#)

Chuang CF, Meyerowitz EM. 2000. Specific and heritable genetic interference by double-stranded RNA in *Arabidopsis thaliana*. *Proc Natl Acad Sci U S A* 97(9): 4985-4990.

Pubmed: [Author and Title](#)

CrossRef: [Author and Title](#)

Google Scholar: [Author Only Title Only Author and Title](#)

Dong Z, Han MH, Fedoroff N. 2008. The RNA-binding proteins HYL1 and SE promote accurate in vitro processing of pri-miRNA by DCL1. *Proc Natl Acad Sci U S A* 105(29): 9970-9975.

Pubmed: [Author and Title](#)

CrossRef: [Author and Title](#)

Google Scholar: [Author Only Title Only Author and Title](#)

Engelsberger WR, Schulze WX. 2012. Nitrate and ammonium lead to distinct global dynamic phosphorylation patterns when resupplied to nitrogen-starved *Arabidopsis* seedlings. *Plant J* 69(6): 978-995.

Pubmed: [Author and Title](#)

CrossRef: [Author and Title](#)

Google Scholar: [Author Only Title Only Author and Title](#)

Fang X, Cui Y, Li Y, Qi Y. 2015. Transcription and processing of primary microRNAs are coupled by Elongator complex in *Arabidopsis*. *Nat Plants* 1: 15075.

Pubmed: [Author and Title](#)

CrossRef: [Author and Title](#)

Google Scholar: [Author Only Title Only Author and Title](#)

Fei Q, Xia R, Meyers BC (2013) Phased, secondary small interfering RNAs in posttranscriptional regulatory networks. *Plant Cell* 25:

Copyright © 2018 American Society of Plant Biologists. All rights reserved.

Pubmed: [Author and Title](#)CrossRef: [Author and Title](#)Google Scholar: [Author Only Title Only Author and Title](#)

Feng B, Ma S, Chen S, Zhu N, Zhang S, Yu B, Yu Y, Le B, Chen X, Dinesh-Kumar SP, Shan L, He P. 2016. PARylation of the forkhead-associated domain protein DAWdle regulates plant immunity. *EMBO Rep* 17(12): 1799-1813.

Pubmed: [Author and Title](#)CrossRef: [Author and Title](#)Google Scholar: [Author Only Title Only Author and Title](#)

Gregory BD, O'Malley RC, Lister R, Urich MA, Tonti-Filippini J, Chen H, Millar AH, Ecker JR. 2008. A link between RNA metabolism and silencing affecting *Arabidopsis* development. *Dev Cell* 14(6): 854-866.

Pubmed: [Author and Title](#)CrossRef: [Author and Title](#)Google Scholar: [Author Only Title Only Author and Title](#)

Grigg SP, Canales C, Hay A, Tsiantis M. 2005. SERRATE coordinates shoot meristem function and leaf axial patterning in *Arabidopsis*. *Nature* 437(7061): 1022-1026.

Pubmed: [Author and Title](#)CrossRef: [Author and Title](#)Google Scholar: [Author Only Title Only Author and Title](#)

Karlsson P, Christie MD, Seymour DK, Wang H, Wang X, Hagmann J, Kulcheski F, Manavella PA. 2015. KH domain protein RCF3 is a tissue-biased regulator of the plant miRNA biogenesis cofactor HYL1. *Proc Natl Acad Sci U S A* 112(45): 14096-14101.

Pubmed: [Author and Title](#)CrossRef: [Author and Title](#)Google Scholar: [Author Only Title Only Author and Title](#)

Kim YJ, Zheng B, Yu Y, Won SY, Mo B, Chen X. 2011. The role of Mediator in small and long noncoding RNA production in *Arabidopsis thaliana*. *EMBO J* 30(5): 814-822.

Pubmed: [Author and Title](#)CrossRef: [Author and Title](#)Google Scholar: [Author Only Title Only Author and Title](#)

Koster T, Meyer K, Weinholdt C, Smith LM, Lummer M, Speth C, Grosse I, Weigel D, Staiger D. 2014. Regulation of pri-miRNA processing by the hnRNP-like protein AtGRP7 in *Arabidopsis*. *Nucleic Acids Res* 42(15): 9925-9936.

Pubmed: [Author and Title](#)CrossRef: [Author and Title](#)Google Scholar: [Author Only Title Only Author and Title](#)

Langmead B, Trapnell C, Pop M, Salzberg SL. 2009. Ultrafast and memory-efficient alignment of short DNA sequences to the human genome. *Genome Biol* 10(3): R25.

Pubmed: [Author and Title](#)CrossRef: [Author and Title](#)Google Scholar: [Author Only Title Only Author and Title](#)

Laubinger S, Sachsenberg T, Zeller G, Busch W, Lohmann JU, Ratsch G, Weigel D. 2008. Dual roles of the nuclear cap-binding complex and SERRATE in pre-mRNA splicing and microRNA processing in *Arabidopsis thaliana*. *Proc Natl Acad Sci U S A* 105(25): 8795-8800.

Pubmed: [Author and Title](#)CrossRef: [Author and Title](#)Google Scholar: [Author Only Title Only Author and Title](#)

Law JA, Jacobsen SE. 2010. Establishing, maintaining and modifying DNA methylation patterns in plants and animals. *Nat Rev Genet* 11(3): 204-220.

Pubmed: [Author and Title](#)CrossRef: [Author and Title](#)Google Scholar: [Author Only Title Only Author and Title](#)

Li S, Liu K, Zhang S, Wang X, Rogers K, Ren G, Zhang C, Yu B. 2017. STV1, a ribosomal protein, binds primary microRNA transcripts to promote their interaction with the processing complex in *Arabidopsis*. *Proc Natl Acad Sci U S A* 114(6): 1424-1429.

Pubmed: [Author and Title](#)CrossRef: [Author and Title](#)Google Scholar: [Author Only Title Only Author and Title](#)

Li S, Liu K, Zhou B, Li M, Zhang S, Zeng L, Zhang C, Yu B (2018) MAC3A and MAC3B, Two Core Subunits of the MOS4-Associated Complex, Positively Influence miRNA Biogenesis. *Plant Cell* 30: 481-494

Pubmed: [Author and Title](#)CrossRef: [Author and Title](#)Google Scholar: [Author Only Title Only Author and Title](#)

Liu C, Axtell MJ, Fedoroff NV. 2012. The helicase and RNaseIII domains of *Arabidopsis* Dicer-Like1 modulate catalytic parameters during microRNA biogenesis. *Plant Physiol* 159(2): 748-758.

Pubmed: [Author and Title](#)CrossRef: [Author and Title](#)

Google Scholar: [Author Only](#) [Title Only](#) [Author and Title](#)

Machida S, Yuan YA. 2013. Crystal structure of *Arabidopsis thaliana* Dawdle forkhead-associated domain reveals a conserved phospho-threonine recognition cleft for dicer-like 1 binding. *Mol Plant* 6(4): 1290-1300.

Pubmed: [Author and Title](#)

CrossRef: [Author and Title](#)

Google Scholar: [Author Only](#) [Title Only](#) [Author and Title](#)

Matzke MA, Mosher RA. 2014. RNA-directed DNA methylation: an epigenetic pathway of increasing complexity. *Nat Rev Genet* 15(6): 394-408.

Pubmed: [Author and Title](#)

CrossRef: [Author and Title](#)

Google Scholar: [Author Only](#) [Title Only](#) [Author and Title](#)

Morris ER, Chevalier D, Walker JC. 2006. DAWDLE, a forkhead-associated domain gene, regulates multiple aspects of plant development. *Plant Physiol* 141(3): 932-941.

Pubmed: [Author and Title](#)

CrossRef: [Author and Title](#)

Google Scholar: [Author Only](#) [Title Only](#) [Author and Title](#)

Mourrain P, Beclin C, Elmayan T, Feuerbach F, Godon C, Morel JB, Jouette D, Lacombe AM, Nikic S, Picault N, Remoue K, Sanial M, Vo TA, Vaucheret H. 2000. *Arabidopsis SGS2* and *SGS3* genes are required for posttranscriptional gene silencing and natural virus resistance. *Cell* 101(5): 533-542.

Pubmed: [Author and Title](#)

CrossRef: [Author and Title](#)

Google Scholar: [Author Only](#) [Title Only](#) [Author and Title](#)

Narayanan L, Mukherjee D, Zhang S, Yu B, Chevalier D. 2014. Mutational analyses of a ForkHead Associated domain protein, DAWDLE, in *Arabidopsis thaliana*. *American Journal of Plant Sciences* 5: 2811-2822.

Pubmed: [Author and Title](#)

CrossRef: [Author and Title](#)

Google Scholar: [Author Only](#) [Title Only](#) [Author and Title](#)

Ossowski S, Schwab R, Weigel D. 2008. Gene silencing in plants using artificial microRNAs and other small RNAs. *Plant J* 53(4): 674-690.

Pubmed: [Author and Title](#)

CrossRef: [Author and Title](#)

Google Scholar: [Author Only](#) [Title Only](#) [Author and Title](#)

Qi Y, Denli AM, Hannon GJ. 2005. Biochemical specialization within *Arabidopsis* RNA silencing pathways. *Mol Cell* 19(3): 421-428.

Pubmed: [Author and Title](#)

CrossRef: [Author and Title](#)

Google Scholar: [Author Only](#) [Title Only](#) [Author and Title](#)

Ren G, Xie M, Dou Y, Zhang S, Zhang C, Yu B. 2012. Regulation of miRNA abundance by RNA binding protein TOUGH in *Arabidopsis*. *Proc Natl Acad Sci U S A* 109(31): 12817-12821.

Pubmed: [Author and Title](#)

CrossRef: [Author and Title](#)

Google Scholar: [Author Only](#) [Title Only](#) [Author and Title](#)

Robinson MD, McCarthy DJ, Smyth GK. 2010. edgeR: a Bioconductor package for differential expression analysis of digital gene expression data. *Bioinformatics* 26(1): 139-140.

Pubmed: [Author and Title](#)

CrossRef: [Author and Title](#)

Google Scholar: [Author Only](#) [Title Only](#) [Author and Title](#)

Robinson MD, Oshlack A. 2010. A scaling normalization method for differential expression analysis of RNA-seq data. *Genome Biol* 11(3): R25.

Pubmed: [Author and Title](#)

CrossRef: [Author and Title](#)

Google Scholar: [Author Only](#) [Title Only](#) [Author and Title](#)

Shahid S, Axtell MJ. 2014. Identification and annotation of small RNA genes using ShortStack. *Methods* 67(1): 20-27.

Pubmed: [Author and Title](#)

CrossRef: [Author and Title](#)

Google Scholar: [Author Only](#) [Title Only](#) [Author and Title](#)

Speth C, Willing EM, Rausch S, Schneeberger K, Laubinger S. 2013. RACK1 scaffold proteins influence miRNA abundance in *Arabidopsis*. *Plant J* 76(3): 433-445.

Pubmed: [Author and Title](#)

CrossRef: [Author and Title](#)

Google Scholar: [Author Only](#) [Title Only](#) [Author and Title](#)

Vaucheret H. 2008. Plant ARGONAUTES. *Trends Plant Sci* 13(7): 350-358.

Pubmed: [Author and Title](#)

CrossRef: [Author and Title](#)

Google Scholar: [Author Only](#) [Title Only](#) [Author and Title](#)

Vaucheret H, Fagard M. 2001. Transcriptional gene silencing in plants: targets, inducers and regulators. Trends Genet 17(1): 29-35.

Pubmed: [Author and Title](#)

CrossRef: [Author and Title](#)

Google Scholar: [Author Only](#) [Title Only](#) [Author and Title](#)

Voinnet O. 2009. Origin, biogenesis, and activity of plant microRNAs. Cell 136(4): 669-687.

Pubmed: [Author and Title](#)

CrossRef: [Author and Title](#)

Google Scholar: [Author Only](#) [Title Only](#) [Author and Title](#)

Wang L, Song X, Gu L, Li X, Cao S, Chu C, Cui X, Chen X, Cao X. 2013. NOT2 proteins promote polymerase II-dependent transcription and interact with multiple MicroRNA biogenesis factors in *Arabidopsis*. Plant Cell 25(2): 715-727.

Pubmed: [Author and Title](#)

CrossRef: [Author and Title](#)

Google Scholar: [Author Only](#) [Title Only](#) [Author and Title](#)

Wu X, Shi Y, Li J, Xu L, Fang Y, Li X, Qi Y. 2013. A role for the RNA-binding protein MOS2 in microRNA maturation in *Arabidopsis*. Cell Res 23(5): 645-657.

Pubmed: [Author and Title](#)

CrossRef: [Author and Title](#)

Google Scholar: [Author Only](#) [Title Only](#) [Author and Title](#)

Xie M, Yu B. 2015. siRNA-directed DNA Methylation in Plants. Curr Genomics 16(1): 23-31.

Pubmed: [Author and Title](#)

CrossRef: [Author and Title](#)

Google Scholar: [Author Only](#) [Title Only](#) [Author and Title](#)

Yoshikawa M, Peragine A, Park MY, Poethig RS. 2005. A pathway for the biogenesis of trans-acting siRNAs in *Arabidopsis*. Genes Dev 19(18): 2164-2175.

Pubmed: [Author and Title](#)

CrossRef: [Author and Title](#)

Google Scholar: [Author Only](#) [Title Only](#) [Author and Title](#)

Yu B, Bi L, Zheng BL, Ji LJ, Chevalier D, Agarwal M, Ramachandran V, Li WX, Lagrange T, Walker JC, Chen XM. 2008. The FHA domain proteins DAWdle in *Arabidopsis* and SNIP1 in humans act in small RNA biogenesis. Proc Natl Acad Sci U S A 105(29): 10073-10078.

Pubmed: [Author and Title](#)

CrossRef: [Author and Title](#)

Google Scholar: [Author Only](#) [Title Only](#) [Author and Title](#)

Zhang X, Lii Y, Wu Z, Polishko A, Zhang H, Chinnusamy V, Lonardi S, Zhu JK, Liu R, Jin H (2013) Mechanisms of small RNA generation from cis-NATs in response to environmental and developmental cues. Mol Plant 6: 704-715

Pubmed: [Author and Title](#)

CrossRef: [Author and Title](#)

Google Scholar: [Author Only](#) [Title Only](#) [Author and Title](#)

Zhan X, Wang B, Li H, Liu R, Kalia RK, Zhu JK, Chinnusamy V. 2012. *Arabidopsis* proline-rich protein important for development and abiotic stress tolerance is involved in microRNA biogenesis. Proc Natl Acad Sci U S A 109(44): 18198-18203.

Pubmed: [Author and Title](#)

CrossRef: [Author and Title](#)

Google Scholar: [Author Only](#) [Title Only](#) [Author and Title](#)

Zhang S, Liu Y, Yu B. 2014. PRL1, an RNA-binding protein, positively regulates the accumulation of miRNAs and siRNAs in *Arabidopsis*. PLoS Genet 10(12): e1004841.

Pubmed: [Author and Title](#)

CrossRef: [Author and Title](#)

Google Scholar: [Author Only](#) [Title Only](#) [Author and Title](#)

Zhang S, Liu Y, Yu B. 2015. New insights into pri-miRNA processing and accumulation in plants. Wiley Interdiscip Rev RNA 6(5): 533-545.

Pubmed: [Author and Title](#)

CrossRef: [Author and Title](#)

Google Scholar: [Author Only](#) [Title Only](#) [Author and Title](#)

Zhang S, Xie M, Ren G, Yu B. 2013. CDC5, a DNA binding protein, positively regulates posttranscriptional processing and/or transcription of primary microRNA transcripts. Proc Natl Acad Sci U S A 110(43): 17588-17593.

Pubmed: [Author and Title](#)

CrossRef: [Author and Title](#)

Google Scholar: [Author Only](#) [Title Only](#) [Author and Title](#)